

~~CONFIDENTIAL~~

C.1 Copy
RM L51C23

NACA RM L51C23

JUN 22 1951



RESEARCH MEMORANDUM

FLIGHT MEASUREMENTS WITH THE DOUGLAS D-558-II

(BUAERO NO. 37974) RESEARCH AIRPLANE

DYNAMIC LATERAL STABILITY

By W. H. Stillwell and J. V. Wilmerding

Langley Aeronautical Laboratory
Langley Field, Va.

CLASSIFICATION CHANGED

UNCLASSIFIED

To _____

By authority of *NACA Res abs* *Effective*
CLASSIFIED DOCUMENT of *4 RN-115* Date *5-8-57*

This document contains classified information affecting the National Defense of the United States within the meaning of the Espionage Act, USC 5031 and 5032. Its transmission or the revelation of its contents in any manner to an unauthorized person is prohibited by law.
Information so classified may be imparted only to persons in the military and naval services of the United States, appropriate civilian officers and employees of the Federal Government who have a legitimate interest therein, and to United States citizens of known loyalty and discretion who of necessity must be informed thereof.

at 5-23-57

NATIONAL ADVISORY COMMITTEE FOR AERONAUTICS

WASHINGTON
June 18, 1951

NACA LIBRARY
LANGLEY AERONAUTICAL LABORATORY
Langley Field, Va.

~~CONFIDENTIAL~~



NATIONAL ADVISORY COMMITTEE FOR AERONAUTICS

RESEARCH MEMORANDUM

FLIGHT MEASUREMENTS WITH THE DOUGLAS D-558-II

(BUAERO NO. 37974) RESEARCH AIRPLANE

DYNAMIC LATERAL STABILITY

By W. H. Stillwell and J. V. Wilmerding

SUMMARY

The dynamic lateral stability of the Douglas D-558-II airplane was measured (controls fixed) at calibrated airspeeds from 167 miles per hour to 474 miles per hour. In the clean condition the damping was light and decreased with the amplitude of the oscillation; and at low amplitudes the damping was essentially zero and hence resulted in an oscillation of small and constant amplitude. In the landing condition, at speeds below 205 miles per hour, the damping was also light, but positive. Above 205 miles per hour in the landing condition, however, there was no measurable damping of the lateral oscillation.

The landing condition lateral oscillation is particularly objectionable to the pilot because of the inherent lack of dynamic stability and the difficulty the pilot experienced in stopping the oscillation. The airplane does not meet the Bureau of Aeronautics' criterion for satisfactory damping of the lateral oscillation in the flight conditions of this investigation.

INTRODUCTION

The NACA is conducting a flight research program utilizing the Douglas D-558-II (BuAero No. 37974) research airplane at the NACA High Speed Flight Research Station, Edwards Air Force Base, Muroc, California. The D-558-II airplanes were designed for flight research in the transonic speed range and were procured for the NACA by the Bureau of Aeronautics of the Navy Department. The flight research program conducted with the BuAero No. 37974 airplane consisted of determining the stability and control characteristics and the aerodynamic loads acting on the wing



and horizontal tail from the stalling speed up to a Mach number of about 0.90. Presented in this paper are the results of an investigation made to determine the dynamic lateral stability characteristics of the airplane. References 1 to 5 present results which have been obtained during the present flight research program on other aerodynamic characteristics of the D-558-II airplane.

SYMBOLS AND COEFFICIENTS

H	pressure altitude, feet
S	wing area, square feet
\bar{c}	mean aerodynamic chord, feet
v	sideslip velocity along Y-axis, feet per second
V_C	calibrated indicated airspeed, miles per hour
V	airspeed, feet per second
b	wing span, feet
q	dynamic pressure, pounds per square foot
ρ	air density, slugs per cubic foot
W	weight, pounds
g	acceleration of gravity, feet per second per second
m	mass, slugs (W/g)
μ_b	relative-density factor based on wing span ($m/\rho S b$)
i_w	wing incidence, degrees
α	angle of attack, degrees
δ_e	elevator position, degrees
δ_a	total aileron position, degrees
δ_r	rudder position, degrees

- η angle of attack of principal longitudinal axis of airplane, positive when principal axis is above flight path at the nose (fig. 1), degrees
- ϵ angle between reference axis and principal axis, positive when reference axis is above principal axis at the nose (fig. 1), degrees
- θ angle between reference axis and horizontal axis, positive when reference axis is above horizontal axis at the nose (fig. 1), degrees
- γ angle between flight path and horizontal, positive in a climb (fig. 1), degrees
- ψ angle of azimuth, radians
- β angle of sideslip $\left(\sin^{-1} \frac{v}{V}\right)$, degrees or radians
- ϕ angle of bank, radians (fig. 2)
- k_{X_0} radius of gyration about principal longitudinal axis, feet
- k_{Z_0} radius of gyration about principal vertical axis, feet
- K_{X_0} nondimensional radius of gyration about principal longitudinal axis $\left(k_{X_0}/b\right)$
- K_{Z_0} nondimensional radius of gyration about principal vertical axis $\left(k_{Z_0}/b\right)$
- K_X nondimensional radius of gyration about longitudinal stability axis $\left(\sqrt{K_{X_0}^2 \cos^2 \eta + K_{Z_0}^2 \sin^2 \eta}\right)$
- K_Z nondimensional radius of gyration about vertical stability axis $\left(\sqrt{K_{Z_0}^2 \cos^2 \eta + K_{X_0}^2 \sin^2 \eta}\right)$

K_{XZ}	nondimensional product-of-inertia parameter $\left((K_{Z_0}^2 - K_{X_0}^2) \cos \eta \sin \eta \right)$
C_{N_A}	airplane normal-force coefficient
C_L	lift coefficient (Lift/qS)
C_n	yawing-moment coefficient (Yawing moment/qSb)
C_l	rolling-moment coefficient (Rolling moment/qSb)
C_Y	lateral-force coefficient (Lateral force/qS)
C_{Y_β}	rate of change of lateral-force coefficient with angle of sideslip, per degree or per radian, as specified $\left(\frac{\partial C_Y}{\partial \beta} \right)$
C_{n_β}	rate of change of yawing-moment coefficient with angle of sideslip, per degree or per radian, as specified $\left(\frac{\partial C_n}{\partial \beta} \right)$
C_{l_β}	rate of change of rolling-moment coefficient with angle of sideslip, per degree or per radian, as specified $\left(\frac{\partial C_l}{\partial \beta} \right)$
C_{Y_p}	rate of change of lateral-force coefficient with rolling-angular-velocity factor, per radian $\left(\frac{\partial C_Y}{\partial \frac{pb}{2V}} \right)$
C_{l_p}	rate of change of rolling-moment coefficient with rolling-angular-velocity factor, per radian $\left(\frac{\partial C_l}{\partial \frac{pb}{2V}} \right)$
C_{n_p}	rate of change of yawing-moment coefficient with rolling-angular-velocity factor, per radian $\left(\frac{\partial C_n}{\partial \frac{pb}{2V}} \right)$
C_{l_r}	rate of change of rolling-moment coefficient with yawing-angular-velocity factor, per radian $\left(\frac{\partial C_l}{\partial \frac{rb}{2V}} \right)$

C_{n_r}	rate of change of yawing-moment coefficient with yawing-angular-velocity factor, per radian $\left(\frac{\partial C_n}{r_b \partial 2V}\right)$
C_{Y_r}	rate of change of lateral-force coefficient with yawing-angular-velocity factor, per radian $\left(\frac{\partial C_Y}{r_b \partial 2V}\right)$
l	tail length (distance from airplane center of gravity to the center of pressure of the vertical tail), feet
Z	height of center of pressure of vertical tail above fuselage axis, feet
p	rolling angular velocity, radians per second
r	yawing angular velocity, radians per second
D_b	differential operator $\left(\frac{d}{ds_b}\right)$
s_b	nondimensional time parameter based on span
λ	complex root of stability equation ($c \pm id$)
t	time, seconds
P	period of oscillations, seconds
$T_{1/2}$	time for amplitude of oscillation or spiral mode to change by factor of 2 (positive value indicates a decrease to half amplitude, negative value indicates an increase to double amplitude)
$C_{1/2}$	cycles for amplitude of oscillation or spiral mode to change by a factor of 2, ($T_{1/2}/P$)

AIRPLANE

The Douglas D-558-II airplanes have sweptback wing and tail surfaces and were designed for combination turbojet and rocket power. The airplane used in the present investigation (BuAero No. 37974) does not have

the rocket engine installed. This airplane was powered only by a J-34-WE-40 turbojet engine which exhausts out of the bottom of the fuselage between the wing and the tail. Photographs of the airplane are shown in figures 3 and 4 and a three-view drawing is shown in figure 5. Pertinent airplane dimensions and characteristics are listed in table I.

Both slats and fences are incorporated on the wing of the airplane. The wing slats can be locked in the closed position or they can be unlocked. When the slats are unlocked, the slat position is a function of the angle of attack of the airplane. Also, the slats on the left and right wings are interconnected and therefore, at any time, assume the same position. A section view of the slat and the forward portion of the wing showing the motion of the slat with respect to the wing is shown in figure 6.

The airplane is equipped with an adjustable stabilizer but no means are provided for trimming out aileron or rudder control forces. No aerodynamic balance or control-force booster system is used on any of the controls. Hydraulic dampers are installed on all control surfaces to aid in preventing control-surface flutter. Dive brakes are located on the rear portion of the fuselage.

The variations of rudder, elevator, and aileron position with control position are shown in figures 7, 8, and 9 and the friction in the control systems as measured on the ground under no load is shown in figures 10, 11, and 12. The friction measurements were obtained by measuring the control position and the control force as the controls were deflected slowly. The rate of control deflection was sufficiently low so that the control force resulting from the hydraulic dampers in the control system was negligible.

INSTRUMENTATION

Standard NACA recording instruments were installed in the airplane to measure the following quantities:

- Airspeed
- Altitude
- Elevator and aileron wheel forces
- Rudder pedal force
- Normal, longitudinal, and transverse accelerations
- Rolling, pitching, and yawing velocities
- Sideslip angle
- Stabilizer, elevator, rudder, left and right aileron, and slat positions

A free-swiveling airspeed head was used to measure both static and total pressure. This airspeed head was mounted on a boom 7 feet forward of the nose of the airplane. A vane which was used to measure angle of sideslip was mounted below the same boom $4\frac{1}{2}$ feet forward of the nose of the airplane. (See fig. 3.) The airspeed system was calibrated by the fly-by method at indicated airspeeds down to 225 miles per hour. The static-pressure error at this speed was 3.5 percent of the impact pressure above the free-stream static pressure. Most of the data presented in this paper are for indicated airspeeds less than 225 miles per hour. For these airspeeds the static-pressure error which was present at 225 miles per hour has been applied to the data.

The left and right aileron positions were measured on the control linkage about 1 foot forward of the ailerons. The stabilizer, rudder, and elevator positions were measured at the control surfaces. All control positions were measured perpendicular to the control hinge line.

The sensitivity of the rudder-control-position recorder (0.043 inch of film deflection per degree of rudder deflection) is such that the minimum movement that may be detected is a control-position oscillation of about 0.25° total amplitude.

TESTS, RESULTS, AND DISCUSSION

The dynamic lateral stability of the Douglas D-558-II airplane was measured in control-fixed lateral oscillations in both the clean and the landing configuration. The lateral oscillations were intentionally excited by abrupt rudder deflections; however, in some cases, particularly in the landing configuration, the oscillations were excited by rough air. The lateral oscillations were recorded in the normal-force-coefficient range from 0.1 to 0.66 in the clean condition and from 0.31 to 0.83 in the landing condition. The altitude varied from 5,000 feet to 21,300 feet.

A typical time history of a lateral oscillation in the clean condition at $H = 20,400$ feet and $V_c = 248$ miles per hour induced by the pilot deflecting the rudder and then abruptly returning the control to the original position is presented in figure 13. The period of the oscillation is 2.5 seconds and the time to damp to half amplitude is 5.2 seconds. The records indicate that the damping of the lateral oscillation in the clean condition is low and the damping becomes less as the amplitude of the oscillation is decreased, resulting in a constant amplitude oscillation of about $\pm 1^\circ$ sideslip. This small oscillation is

difficult for the pilot to stop. The records were turned off at 17 seconds so it is not known if the oscillation would have damped completely. Pilot's comments and other data indicate that in the clean condition, especially at high speeds, a constant, small-amplitude oscillation (snaking) sometimes occurred.

A time history of an oscillation in the landing condition at $H = 16,400$ feet and $V_c = 229$ miles per hour (fig. 14) shows that there is no measureable damping in this configuration at this airspeed. The oscillation, once started, persists at constant amplitude but can be reduced to small amplitude by the use of rudder control. The amplitude of this oscillation is considerably greater than that of the residual oscillation obtained in the clean condition. The oscillation can be started by rough air or any small control deflection. Dynamic lateral characteristics such as these would probably be intolerable in a service-type aircraft. In the velocity range below 205 miles per hour in the landing condition, however, the airplane becomes laterally stable although the damping is light.

Figures 15 and 16 show the difficulty of controlling the lateral oscillation in the landing condition with the rudder. The rudder control is effective, but the pilot has difficulty in applying the rudder deflection at the exact moment necessary to stop the oscillation. This is shown in figure 15 where the pilot's control movements are out of phase with the oscillation and the oscillation continues undamped while in figure 16 both rudder and aileron control are applied in the proper phase relationship and the oscillation is damped. Because of this lack of inherent stability and the difficulty of controlling the oscillation, the oscillation in this airplane configuration is objectionable to the pilot. It should be pointed out that the airspeed during the oscillation shown in figure 15 is in the velocity range of no damping (237 mph), while the airspeed during the oscillation in figure 16 is in the range of light damping (205 mph). This may partially account for the ease in controlling the oscillation shown in figure 16.

The pilot's ability to control the lateral oscillation in the landing condition improves greatly with practice and if he makes an effort to lead the yawing motion with rudder control, he is able to damp the oscillation quickly, although continuous control is required. The pilots have developed a technique to use in landing this airplane in which the landing approach is made with the landing gear down and the slats unlocked until the airplane has decelerated to the speed range where the lateral oscillations are damped, at which time the flaps are lowered. This method allows the pilot to make his approach without having to concentrate on controlling the lateral oscillation.

The measured values of period and time to damp to one-half amplitude tabulated in table II are presented as a function of normal-force coefficient in figure 17. Also shown in figure 17 are the predicted values calculated by the method presented in the appendix. The predicted values show good agreement with the measured values of period-damping characteristics for the clean configuration. In the landing condition, however, the predicted values do not agree with the measured values probably because of the difficulty of estimating the stability parameters for the landing configuration and the difficulty of measuring very low values of damping in flight. Also, in both configurations, discrepancies in the time to damp to one-half amplitude may be due to the point that a constant value of μ_b was used in the calculations for each configuration, whereas the experimental values of μ_b varied with altitude and fuel consumption (reference 6).

Figure 18 presents the flight data for the clean configuration compared with the Bureau of Aeronautics' criterion for satisfactory period-damping characteristics as given in reference 7. The airplane does not meet the criterion for satisfactory damping of the lateral oscillation in the flight conditions of this investigation.

CONCLUSIONS

The dynamic lateral stability of the D-558-II airplane was measured (controls fixed) at calibrated airspeeds from 167 to 474 miles per hour. In the clean condition the damping was light and decreased with the amplitude of the oscillation; and at low amplitudes the damping was essentially zero and hence resulted in an oscillation of small and constant amplitude. In the landing condition, at speeds below 205 miles per hour, the damping was also light, but positive. Above 205 miles per hour in the landing condition, however, there was no measurable damping of the lateral oscillation.

The landing-condition lateral oscillation is particularly objectionable to the pilot because of the inherent lack of dynamic stability and the difficulty the pilot experienced in stopping the oscillation. The airplane does not meet the Bureau of Aeronautics' criterion for satisfactory damping of the lateral oscillation in the flight conditions of this investigation.

Langley Aeronautical Laboratory
National Advisory Committee for Aeronautics
Langley Field, Va.

APPENDIX

ESTIMATION OF LATERAL PERIOD AND DAMPING CHARACTERISTICS

The nondimensional lateral equations of motion (reference 8), referred to a stability axes system (fig. 2) and used for predicting the lateral period-damping characteristics of the Douglas D-588-II research airplane with the controls fixed, are:

For roll

$$2\mu_b (K_X^2 D_b^2 \phi + K_{XZ} D_b^2 \psi) = C_{l_\beta} \beta + \frac{1}{2} C_{l_p} D_b \phi + \frac{1}{2} C_{l_r} D_b \psi$$

for yaw

$$2\mu_b (K_Z^2 D_b^2 \psi + K_{XZ} D_b^2 \phi) = C_{n_\beta} \beta + \frac{1}{2} C_{n_p} D_b \phi + \frac{1}{2} C_{n_r} D_b \psi$$

and for sideslip

$$2\mu_b (D_b \beta + D_b \psi) = C_{Y_\beta} \beta + \frac{1}{2} C_{Y_p} D_b \phi + C_L \phi + \frac{1}{2} C_{Y_r} D_b \psi + (C_L \tan \gamma) \psi$$

When $\phi_0 e^{\lambda s_b}$ is substituted for ϕ , $\psi_0 e^{\lambda s_b}$ for ψ , and $\beta_0 e^{\lambda s_b}$ for β in the equations written in determinant form, λ must be a root of the stability equation:

$$A\lambda^4 + B\lambda^3 + C\lambda^2 + D\lambda + E = 0$$

where

$$A = 8\mu_b^3 (K_X^2 K_Z^2 - K_{XZ}^2)$$

$$B = -2\mu_b^2 (2K_X^2 K_Z^2 C_{Y_\beta} + K_X^2 C_{n_r} + K_Z^2 C_{l_p} - 2K_{XZ}^2 C_{Y_\beta} - K_{XZ} C_{l_r} - K_{XZ} C_{n_p})$$

$$\begin{aligned}
C = & \mu_b \left(K_X^2 C_{n_r} C_{Y_\beta} + 4\mu_b K_X^2 C_{n_\beta} + K_Z^2 C_{l_p} C_{Y_\beta} + \frac{1}{2} C_{n_r} C_{l_p} - K_{XZ} C_{l_r} C_{Y_\beta} - \right. \\
& 4\mu_b K_{XZ} C_{l_\beta} - C_{n_p} K_{XZ} C_{Y_\beta} - \frac{1}{2} C_{n_p} C_{l_r} + K_{XZ} C_{n_\beta} C_{Y_p} - \\
& \left. K_Z^2 C_{Y_p} C_{l_\beta} - K_X^2 C_{Y_r} C_{n_\beta} + K_{XZ} C_{Y_r} C_{l_\beta} \right) \\
D = & -\frac{1}{4} C_{n_r} C_{l_p} C_{Y_\beta} - \mu_b C_{l_p} C_{n_\beta} + \frac{1}{4} C_{n_p} C_{l_r} C_{Y_\beta} + \mu_b C_{n_p} C_{l_\beta} + \\
& 2\mu_b C_{l_r} K_{XZ} C_{n_\beta} - 2\mu_b C_{l_r} K_Z^2 C_{l_\beta} - 2\mu_b K_X^2 C_{n_\beta} C_{l_r} \tan \gamma + \\
& 2\mu_b K_{XZ} C_{l_\beta} C_{l_r} \tan \gamma + \frac{1}{4} C_{l_p} C_{n_\beta} C_{Y_r} - \frac{1}{4} C_{n_p} C_{l_\beta} C_{Y_r} - \frac{1}{4} C_{l_r} C_{n_\beta} C_{Y_p} + \\
& \frac{1}{4} C_{n_r} C_{l_\beta} C_{Y_p} \\
E = & \frac{1}{2} C_{l_r} \left(C_{n_r} C_{l_\beta} - C_{l_r} C_{n_\beta} \right) + \frac{1}{2} C_{l_r} \tan \gamma \left(C_{l_p} C_{n_\beta} - C_{n_p} C_{l_\beta} \right)
\end{aligned}$$

The damping and period of the lateral oscillation are given by the equations $T_{1/2} = -\frac{0.69}{c} \frac{b}{V}$, $P = \frac{2\pi}{d} \frac{b}{V}$, and $C_{1/2} = \frac{T_{1/2}}{P}$ where c and d are the real and imaginary parts of the complex root of the stability equations.

The stability equation was solved to determine the period and time to damp to one-half amplitude for each condition. The conditions for which calculations were made are presented in table III. The aerodynamic characteristics of table III used in computing the roots of the stability equations were obtained from wind-tunnel tests where available and those not available were estimated by the method presented in reference 9. The mass characteristics were obtained from the Douglas Company.

REFERENCES

1. Sjoberg, Sigurd A.: Preliminary Measurements of the Dynamic Lateral Stability Characteristics of the Douglas D-558-II (BuAero No. 37974) Airplane. NACA RM L9G18, 1949.
2. Wilmerding, J. V., Stillwell, W. H., and Sjoberg, S. A.: Flight Measurements with the Douglas D-558-II (BuAero No. 37974) Research Airplane. Lateral Control Characteristics as Measured in Abrupt Aileron Rolls at Mach Numbers up to 0.86. NACA RM L50E17, 1950.
3. Mayer, John P., and Valentine, George M.: Flight Measurements with the Douglas D-558-II (BuAero No. 37974) Research Airplane. Measurements of the Buffet Boundary and Peak Airplane Normal-Force Coefficients at Mach Numbers up to 0.90. NACA RM L50E31, 1950.
4. Sjoberg, S. A.: Flight Measurements with the Douglas D-558-II (BuAero No. 37974) Research Airplane. Static Lateral and Directional Stability Characteristics as Measured in Sideslips at Mach Numbers up to 0.87. NACA RM L50C14, 1950.
5. Mayer, John P., Valentine, George M., and Mayer, Geraldine C.: Flight Measurements with the Douglas D-558-II (BuAero No. 37974) Research Airplane. Determination of the Aerodynamic Center and Zero-Lift Pitching-Moment Coefficient of the Wing-Fuselage Combination by Means of Tail-Load Measurements in the Mach Number Range from 0.37 to 0.87. NACA RM L50D10, 1950.
6. Queijo, M. J., and Michael, W. H., Jr.: Analysis of the Effects of Various Mass, Aerodynamic, and Dimensional Parameters on the Dynamic Lateral Stability of the Douglas D-558-2 Airplane. NACA RM L9A24, 1949.
7. Anon.: Specification for Flying Qualities of Piloted Airplanes. NAVAER SR-119B, Bur. Aero., June 1, 1948.
8. Sternfield, Leonard, and Gates, Ordway B., Jr.: A Simplified Method for the Determination and Analysis of the Neutral-Lateral-Oscillatory-Stability Boundary. NACA Rep. 943, 1949. (Formerly NACA TN 1727.)
9. Toll, Thomas A., and Queijo, M. J.: Approximate Relations and Charts for Low-Speed Stability Derivatives of Swept Wings. NACA TN 1581, 1948.

TABLE I
DIMENSIONS AND CHARACTERISTICS OF THE
DOUGLAS D-558-II AIRPLANE

Wing:

Root airfoil section (normal to 0.30 chord)	NACA 63-010
Tip airfoil section (normal to 0.30 chord)	NACA 63 ₁ -012
Total area, sq ft	175.0
Span, ft	25.0
Mean aerodynamic chord, in.	87.301
Root chord (parallel to plane of symmetry), in.	108.508
Tip chord (parallel to plane of symmetry), in.	61.180
Taper ratio	0.565
Aspect ratio	3.570
Sweep at 0.30 chord, deg	35.0
Incidence at fuselage center line, deg	3.0
Dihedral, deg	-3.0
Geometric twist, deg	0
Total aileron area (aft of hinge), sq ft	9.8
Aileron travel (each), deg	+15
Total flap area, sq ft	12.58
Flap travel, deg	50

Horizontal tail:

Root airfoil section (normal to 0.30 chord)	NACA 63-010
Tip airfoil section (normal to 0.30 chord)	NACA 63-010
Area (including fuselage), sq ft	39.9
Span, in.	143.6
Mean aerodynamic chord, in.	41.75
Root chord (parallel to plane of symmetry), in.	53.6
Tip chord (parallel to plane of symmetry), in.	26.8
Taper ratio	0.50
Aspect ratio	3.59
Sweep at 0.30-chord line, deg	40.0
Dihedral, deg	0
Elevator area, sq ft	9.4
Elevator travel, deg.	
Up	25
Down	15
Stabilizer travel, deg	
Leading edge up	4
Leading edge down	5

TABLE I
DIMENSIONS AND CHARACTERISTICS OF THE
DOUGLAS D-558-II AIRPLANE - Concluded

Vertical tail:	
Airfoil section (normal to 0.30 chord)	NACA 63-010
Area, sq ft	36.6
Height from fuselage center line, in.	98.0
Root chord (parallel to fuselage center line), in.	146.0
Tip chord (parallel to fuselage center line), in.	44.0
Sweep angle at 0.30 chord, deg	49.0
Rudder area (aft of hinge line), sq ft	6.15
Rudder travel, deg	±25
Fuselage:	
Length, ft	42.0
Maximum diameter, in.	60.0
Fineness ratio	8.40
Speed-retarder area, sq ft	5.25
Power plant	J-34-WE-40 2 jatos for take-off
Airplane weight (full fuel), lb	10,645
Airplane weight (no fuel), lb	9,085
Airplane weight (full fuel and 2 jatos), lb	11,060
Center-of-gravity locations:	
Full fuel (gear down), percent mean aerodynamic chord	25.3
Full fuel (gear up), percent mean aerodynamic chord	25.8
No fuel (gear down), percent mean aerodynamic chord	26.8
No fuel (gear up), percent mean aerodynamic chord	27.5
Full fuel and 2 jatos (gear down), percent mean aerodynamic chord	29.2

$$\frac{W}{S} = 60 = \frac{10645}{175}$$

$$\frac{I}{x_0} = 3150$$

$$\frac{I}{z_0} = 28000$$



TABLE II
D-558-II AIRPLANE, DYNAMIC-LATERAL-STABILITY
FLIGHT-TEST DATA

Condition	V_c	H	C_{NA}	P	$T_{1/2}$	$C_{1/2}$
Clean	474	13,300	0.11	1.5	3.45	2.3
Clean	355	12,200	.14	1.65	6.25	3.8
Clean	385	12,000	.12	1.65	8	4.85
Clean	375 to 464	19,100 to 14,500	.15 to .11	1.75	6.75	3.86
Clean	315 to 375	21,000 to 19,100	.22 to .15	2.0	5.9	2.95
Clean	385	12,200	.21	1.6	5	3.12
Clean	248	20,400	.37	2.5	5.2	2.08
Clean	230	19,900	.45	2.7	---	---
Clean	207	21,300	.56	3.0	---	---
Clean	188	20,800	.66	3.0	---	---
Landing	263	12,000	.31	2.5	---	---
Landing	246	5,000	.35	2.7	---	---
Landing	240	14,000	.35	2.65	---	---
Landing	237	7,200	.37	2.7	---	---
Landing	232	4,000	.39	2.6	---	---
Landing	229	16,400	.40	2.5	---	---
Landing	215	18,300	.45	3.0	---	---
Landing	205	8,600	.50	3.1	---	---
Landing	200	12,000	.52	3.0	---	---
Landing	174	13,100	.70	3.4	---	---
Landing	172	16,100	.78	3.3	---	---
Landing	167	19,300	.82	3.2	---	---

TABLE III
 STABILITY DERIVATIVES AND MASS CHARACTERISTICS USED IN CALCULATIONS
 OF LATERAL STABILITY OF D-558-II AIRPLANE

Configuration	H (ft)	H _b	$\left(\frac{k_{x_0}}{b}\right)^2$	$\left(\frac{k_{y_0}}{b}\right)^2$	η (deg)	K_X^2 (a)	K_Z^2 (a)	K_{XZ} (a)	C_{l_p} (radians)	C_{l_r} (radians)	C_{l_r} (radians)	C_{n_p} (radians)	C_{n_r} (radians)	C_{Y_p} (radians)	C_{Y_r} (radians)	$\tan \gamma$	C_L	$\frac{m}{\rho S V}$	C_{n_b} (radians)	C_{l_b} (radians)
Clean	20,000	56.1	0.01616	0.1447	3.35	0.01699892	0.1442611	-0.007498428	-0.335	-0.763	0.120	0.070	-0.470	0	0	0	0.15	1.81	0.222	-0.1304
					0	0.01616	.1447	0	-.345	-.762	.146	.042	-.454	0	0	0	.300	2.555	.2178	-.1454
					3.75	.01670984	.1441502	-.008388916	-.350	-.767	.201	-.012	-.396	0	0	0	.60	3.72	.2077	-.1838
Landing	12,000	43.1	.0171	.1447	6.65	.01881119	.1429888	-.01467717	-.355	-.890	.293	.103	-.629	0	0	0	.40	2.58	.290	-.160
					3.25	.01751012	.1442899	-.007222368	-.350	-.907	.329	.060	-.644	0	0	0	.60	3.17	.259	-.177
					3.10	.01710039	.1446996	-.0002226999	-.345	-.930	.358	.017	-.648	0	0	0	.80	3.66	.268	-.196
					3.05	.01746124	.1443388	.00677965	-.340	-.975	.390	-.028	-.644	0	0	0	1.0	4.09	.272	-.244

$$\begin{cases}
 K_X^2 = \left(\frac{k_{x_0}}{b}\right)^2 \cos^2 \eta + \left(\frac{k_{y_0}}{b}\right)^2 \sin^2 \eta \\
 K_Z^2 = \left(\frac{k_{x_0}}{b}\right)^2 \cos^2 \eta + \left(\frac{k_{y_0}}{b}\right)^2 \sin^2 \eta \\
 K_{XZ} = \left[\left(\frac{k_{x_0}}{b}\right)^2 - \left(\frac{k_{y_0}}{b}\right)^2\right] \cos \eta \sin \eta
 \end{cases}$$

NACA

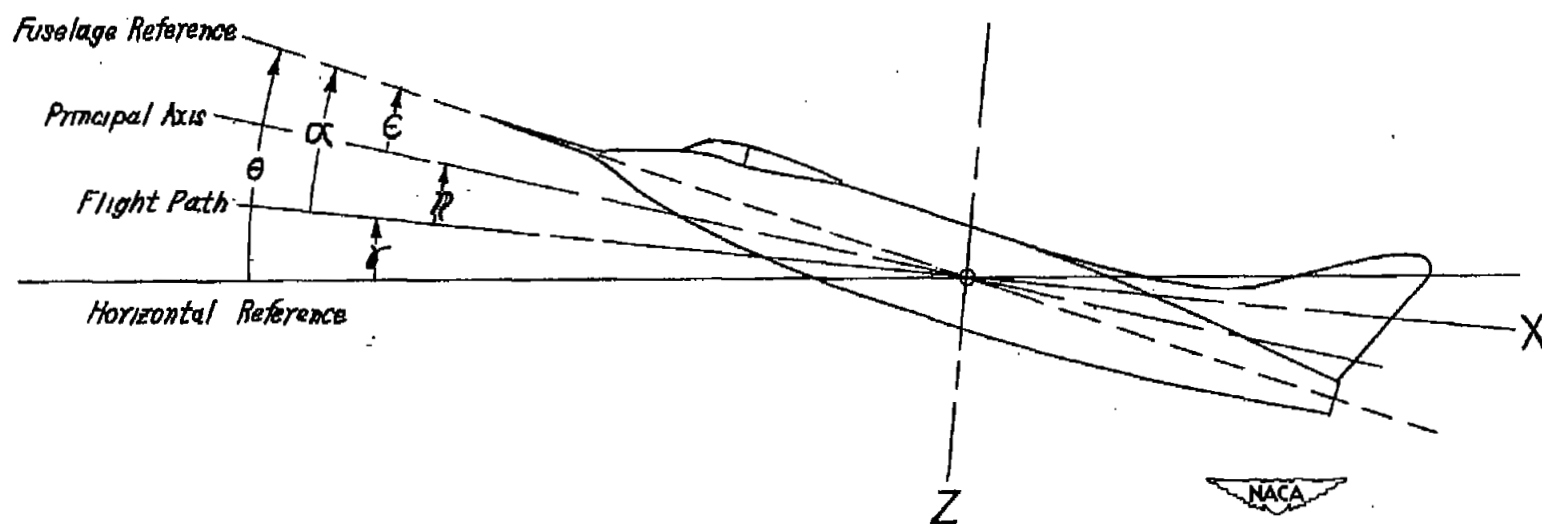


Figure 1.- System of axes and angular relationship in flight. Arrows indicate positive direction of angles. $\eta = \theta - \gamma - \epsilon$.

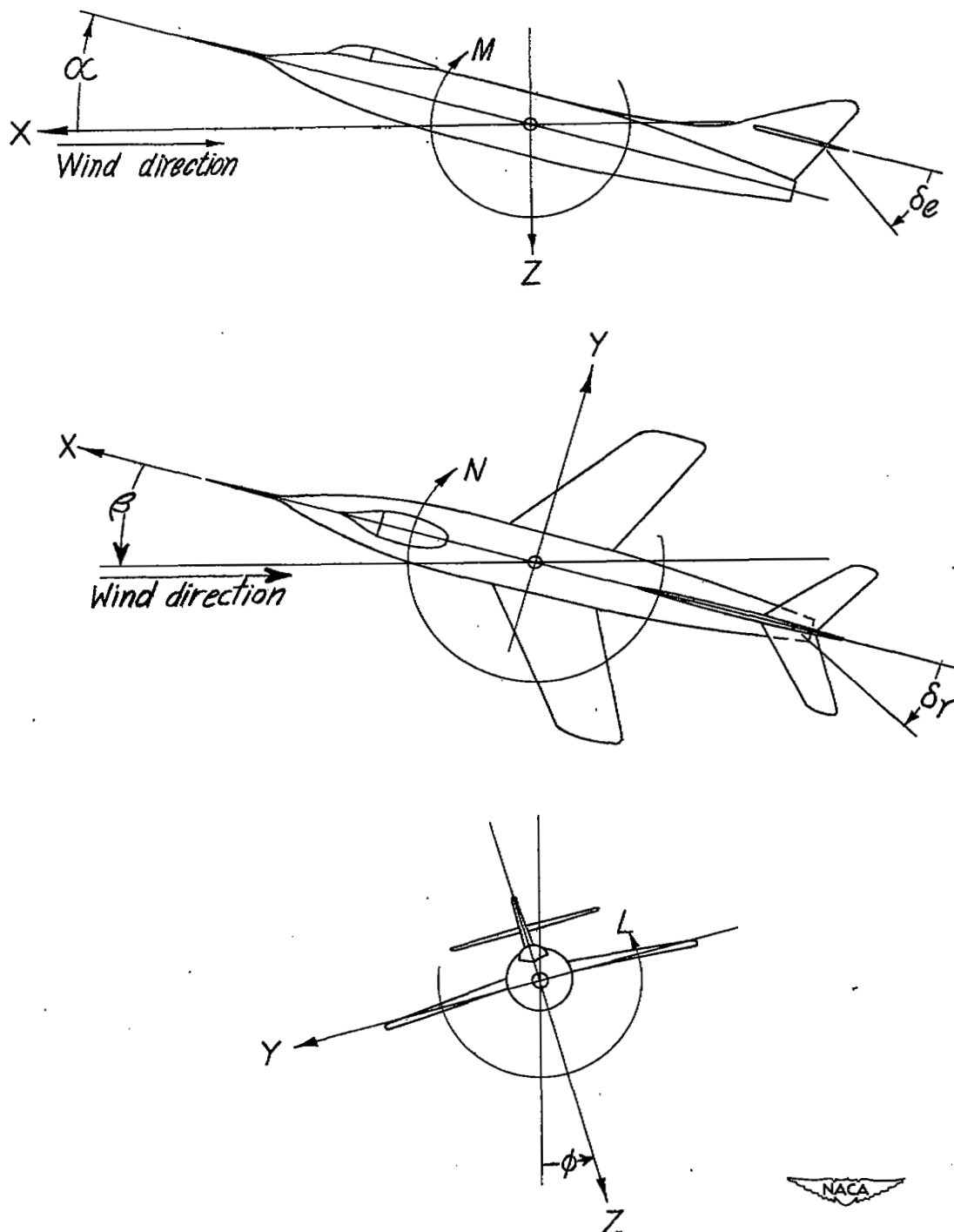


Figure 2.- System of axes and control-surface deflections. Positive values of forces, moments, and angles are indicated by arrows.

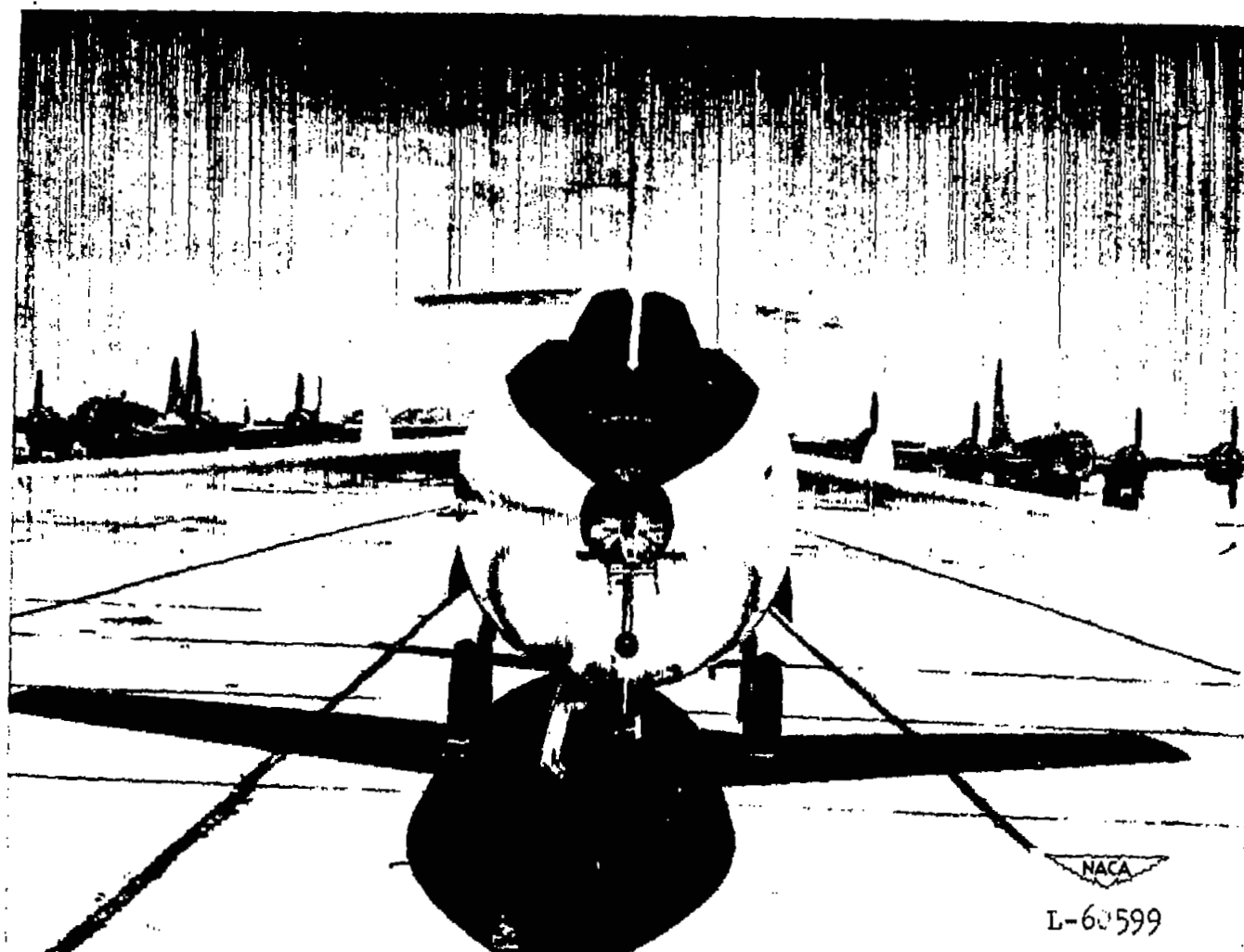
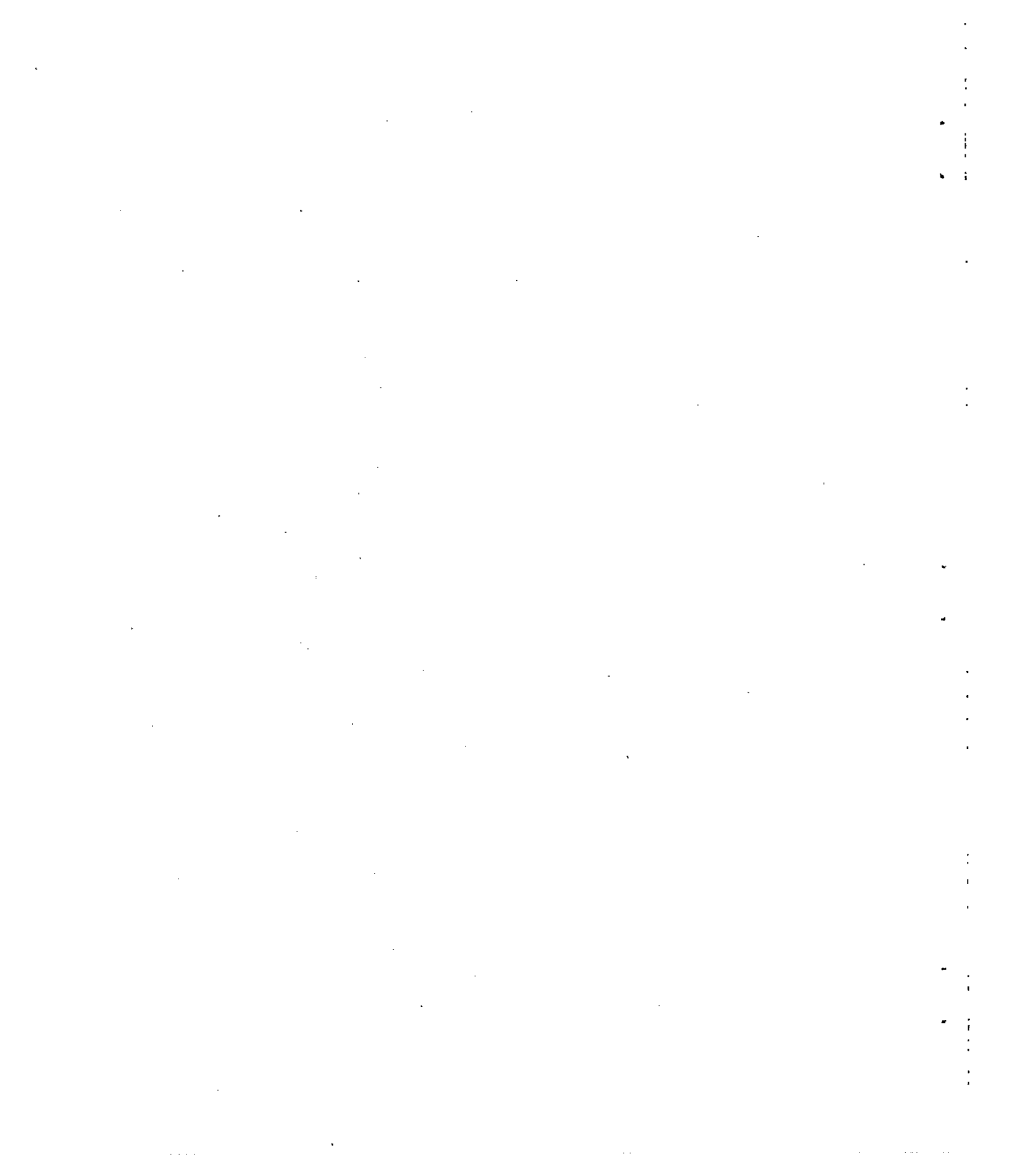


Figure 3.- Front view of Douglas D-558-II (BuAero No. 37974) research airplane.



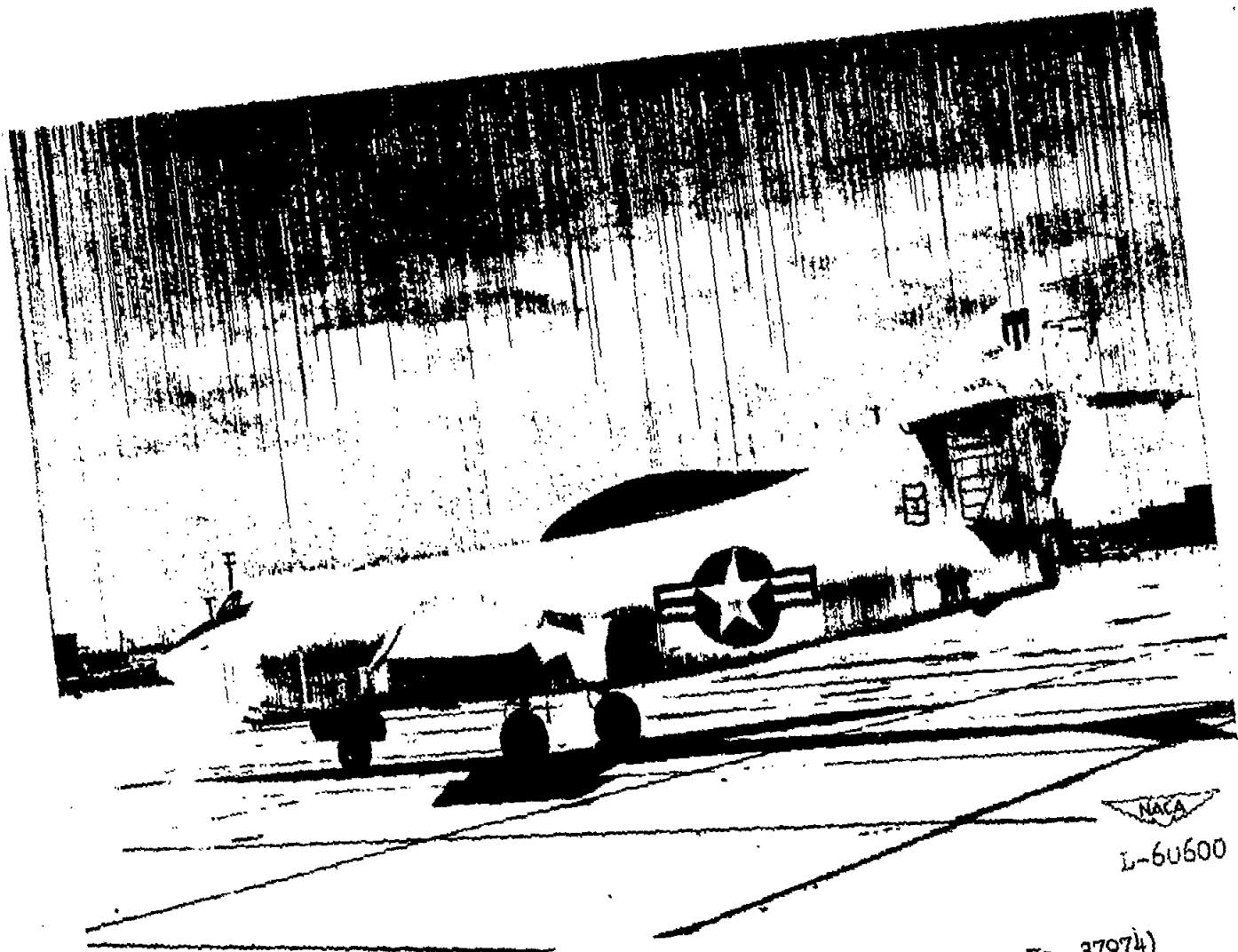
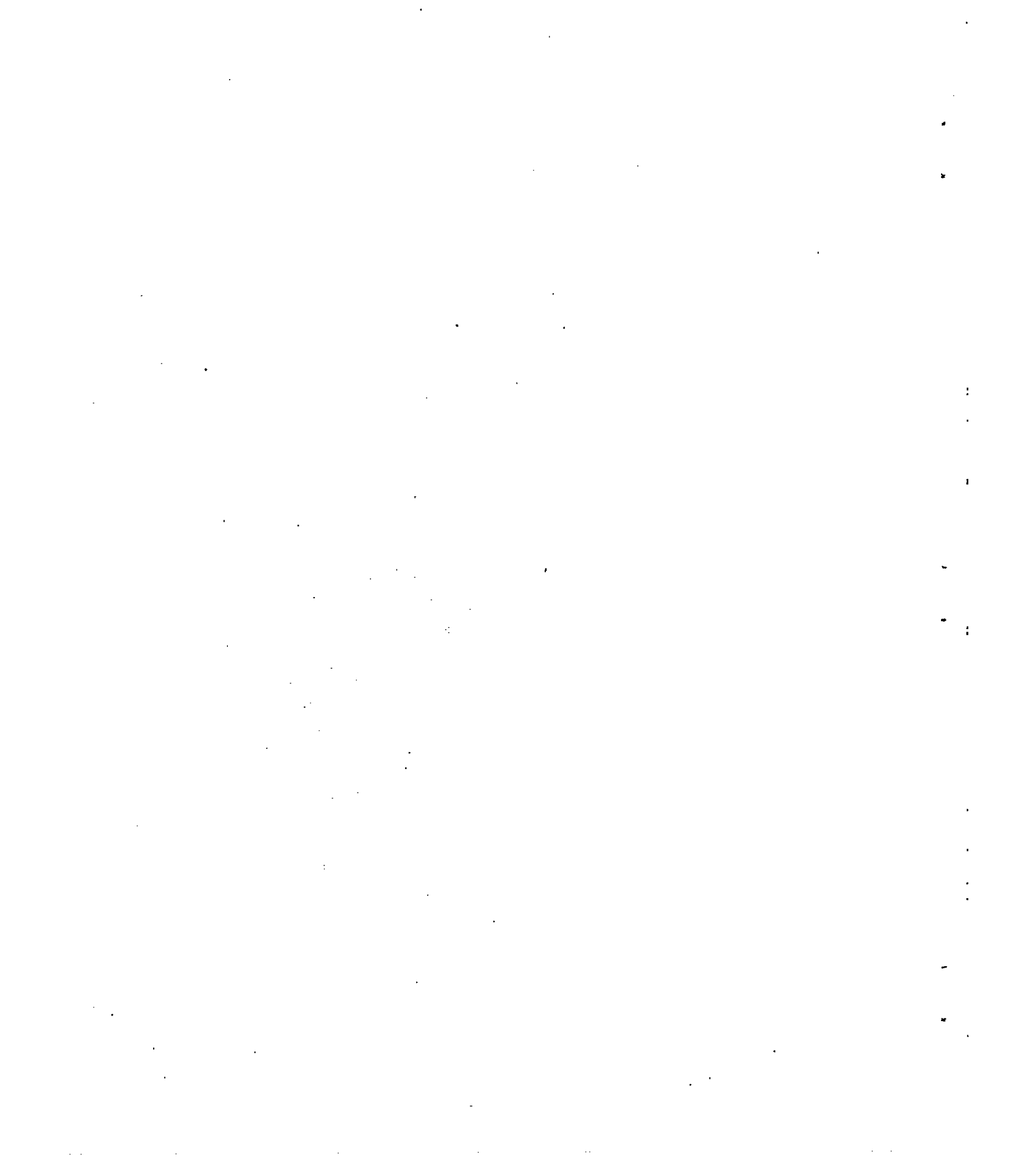


Figure 4.- Three-quarter rear view of Douglas D-558-II (BuAero No. 37974) research airplane.



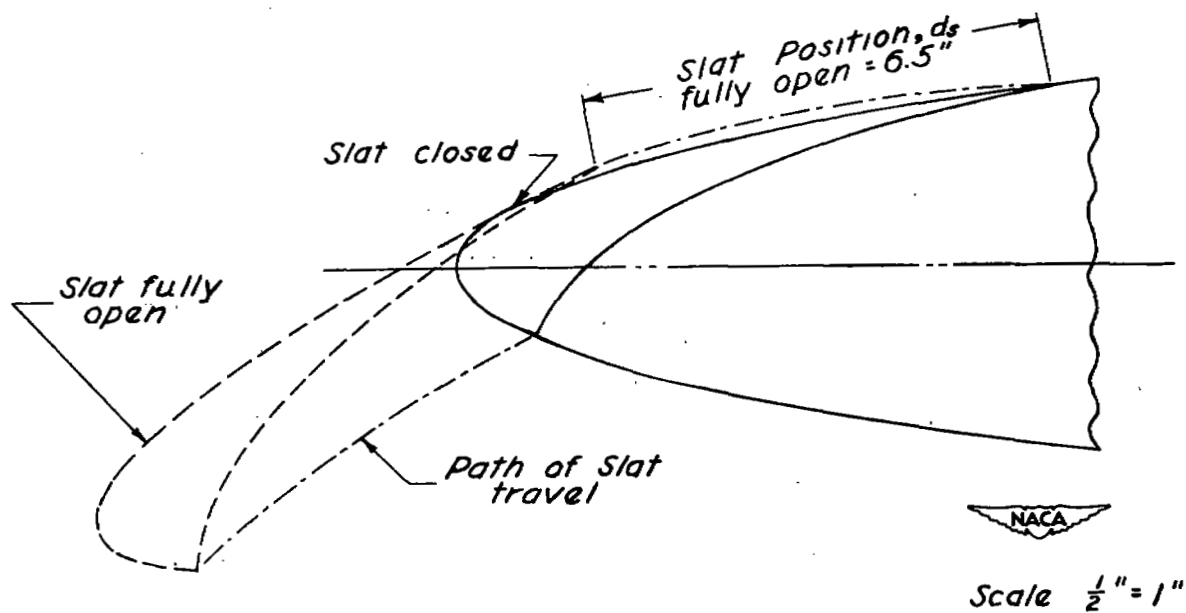


Figure 6.- Section of wing slat of Douglas D-558-II (BuAero No. 37974) research airplane perpendicular to leading edge of wing.

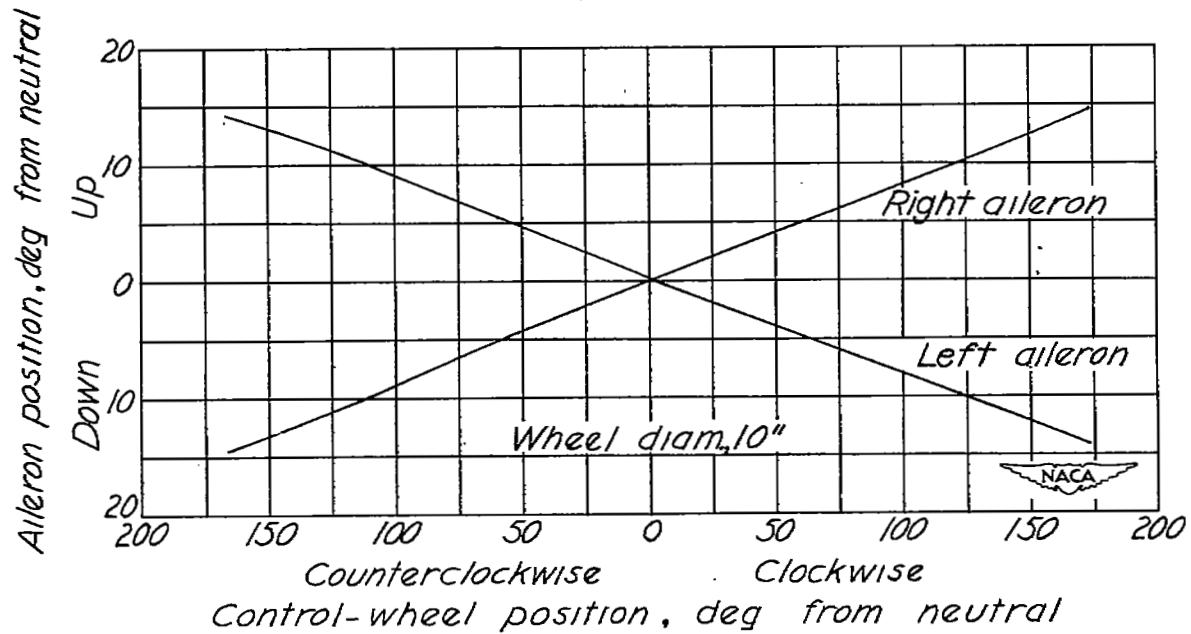


Figure 7.- Variation of left and right aileron positions with control-wheel position. No load on system.

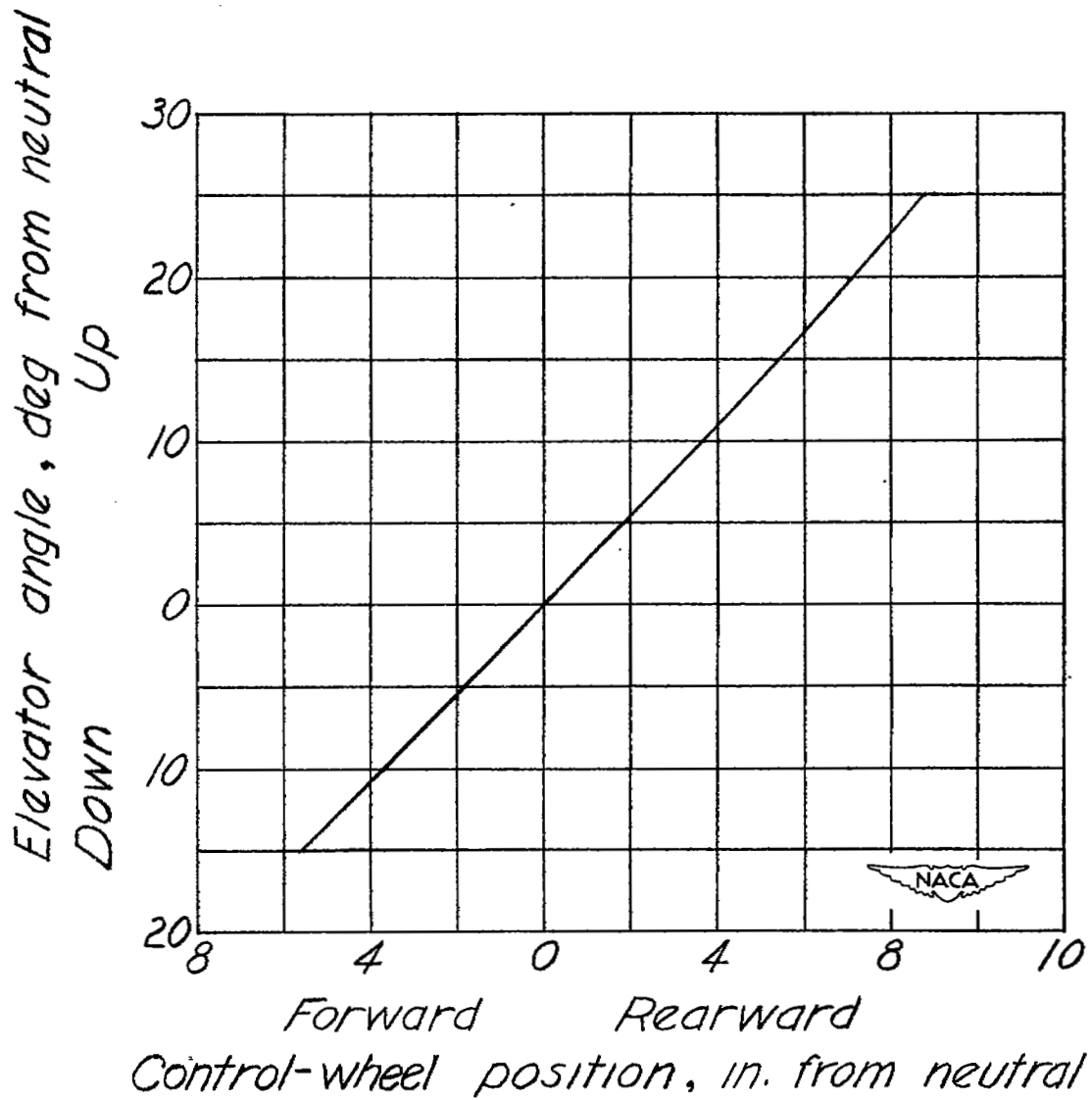


Figure 8.- Variation of elevator position with control-wheel position.
No load on system.

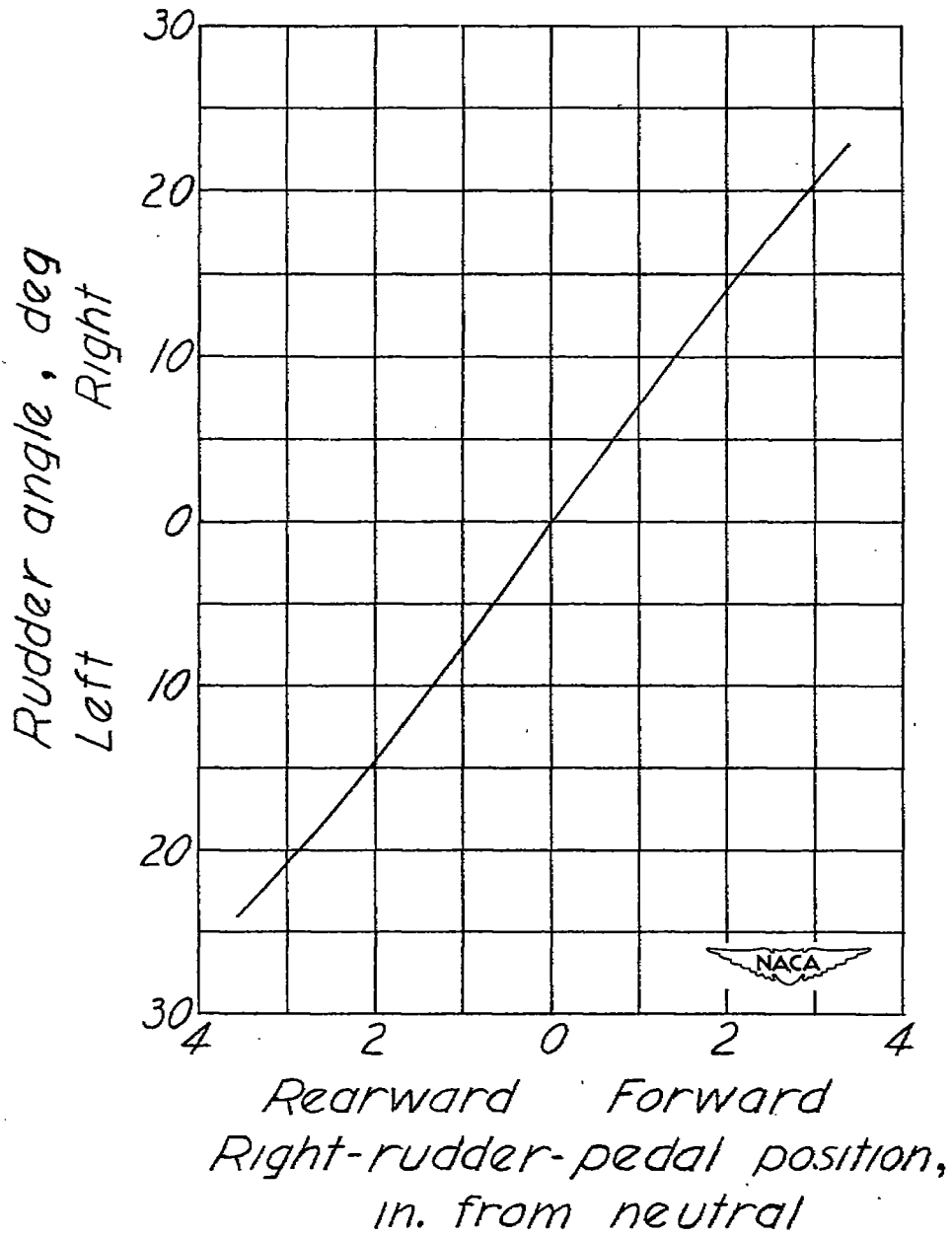


Figure 9.- Variation of rudder position with right-rudder-pedal position.
No load on system.

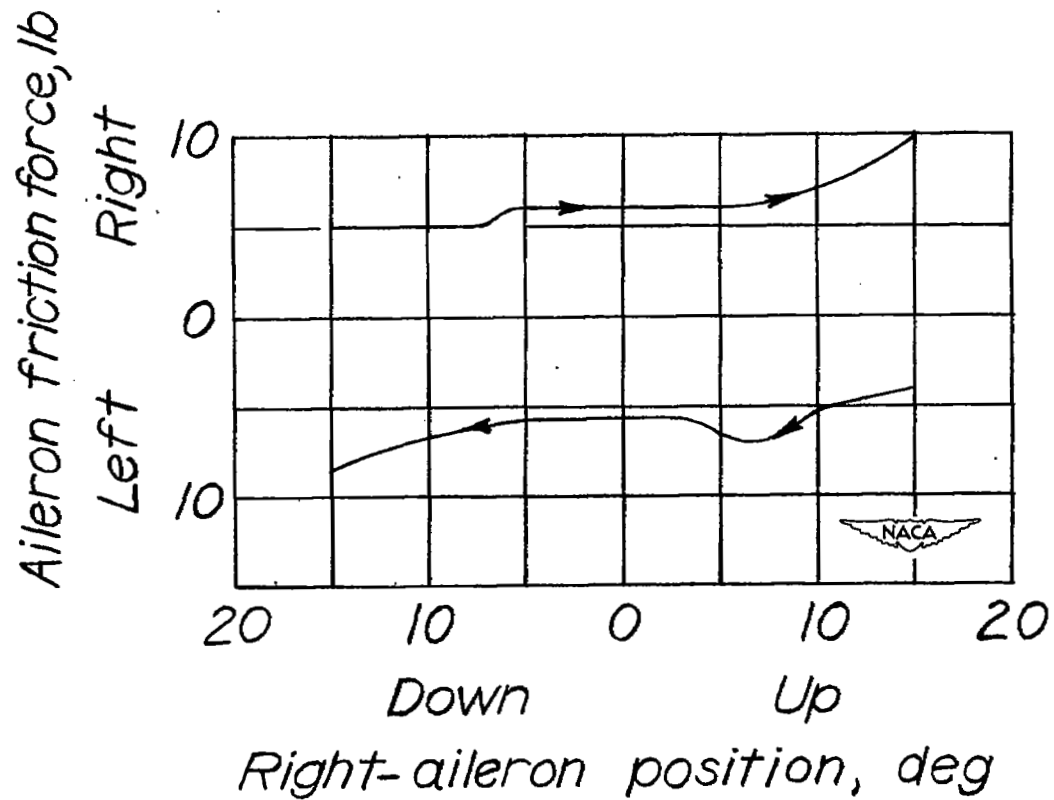


Figure 10.- Aileron-control force required to deflect ailerons on the ground under no load.

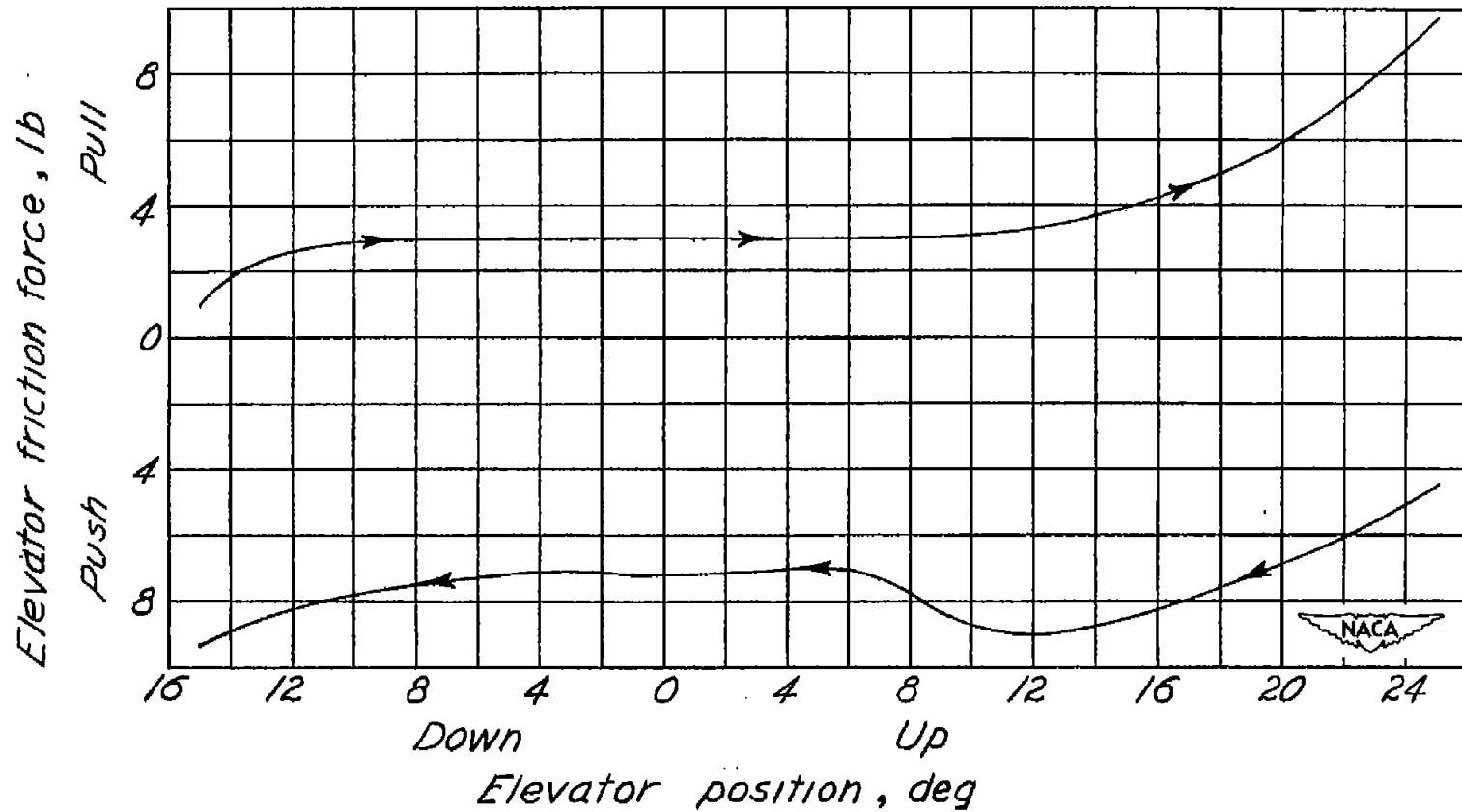


Figure 11.- Elevator-control force required to deflect elevator on the ground under no load.

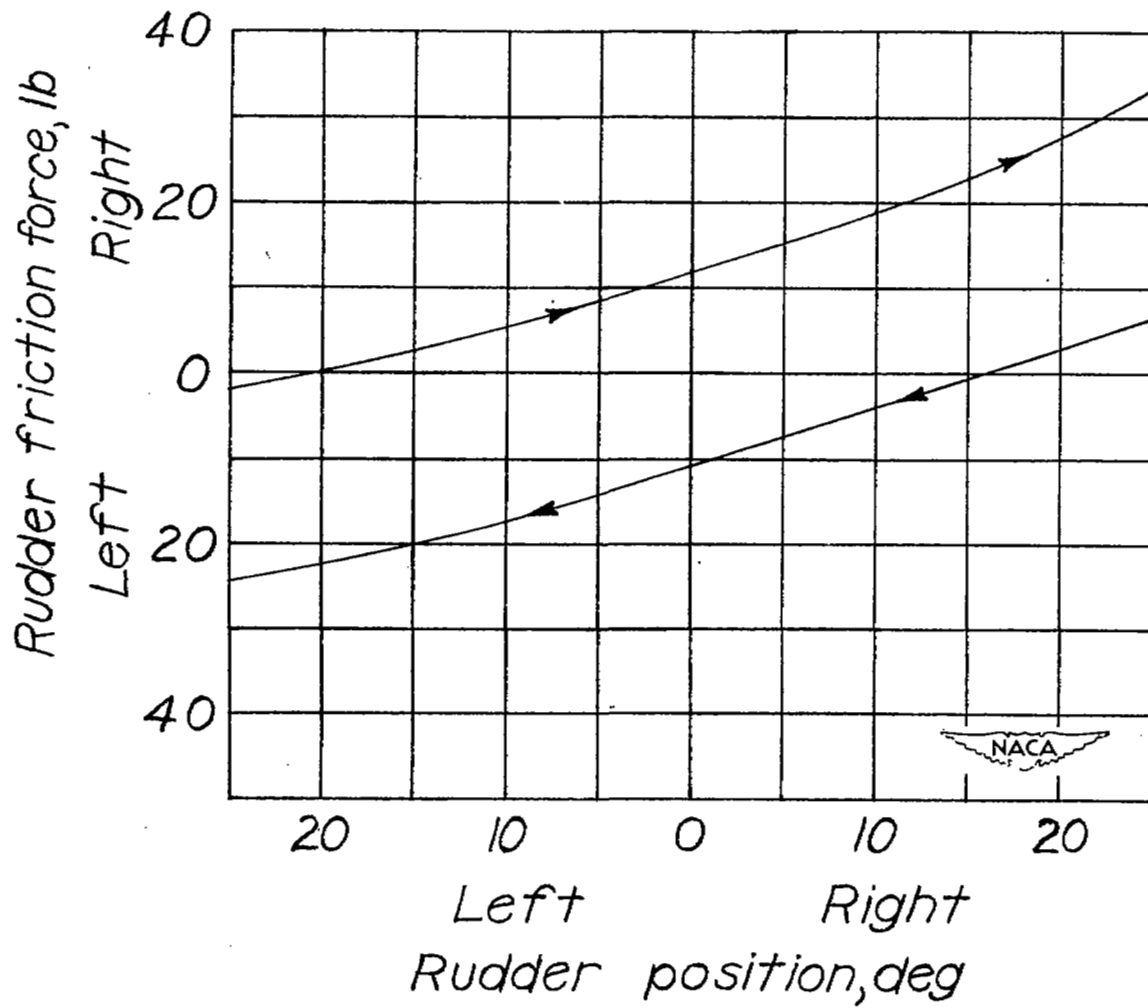


Figure 12.- Rudder-control force required to deflect rudder on the ground under no load.

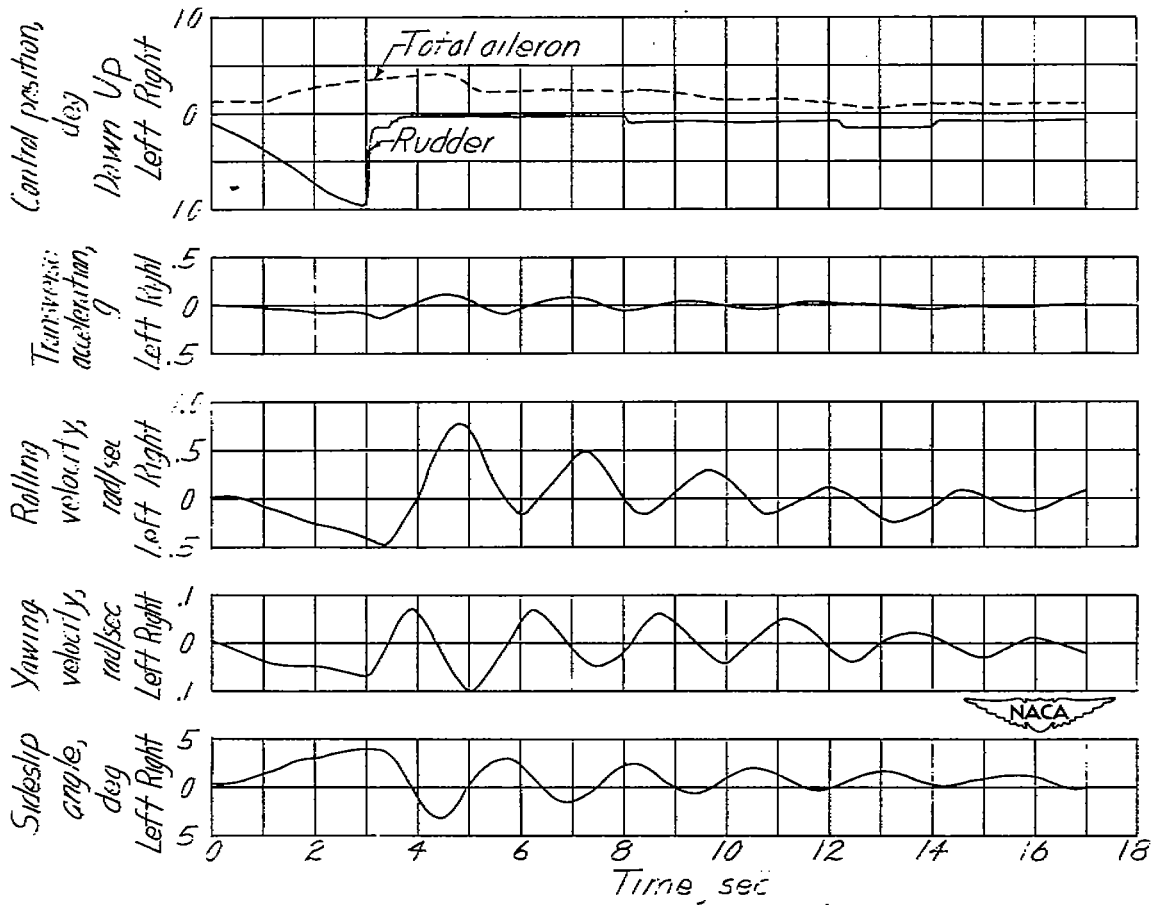


Figure 13.- Time history of a control-fixed lateral oscillation of the D-558-II (BuAero No. 37974) research airplane. Flaps up; landing gear up; slats locked; $V_c = 248$ miles per hour; $H = 20,400$ feet; $C_{NA} = 0.37$.

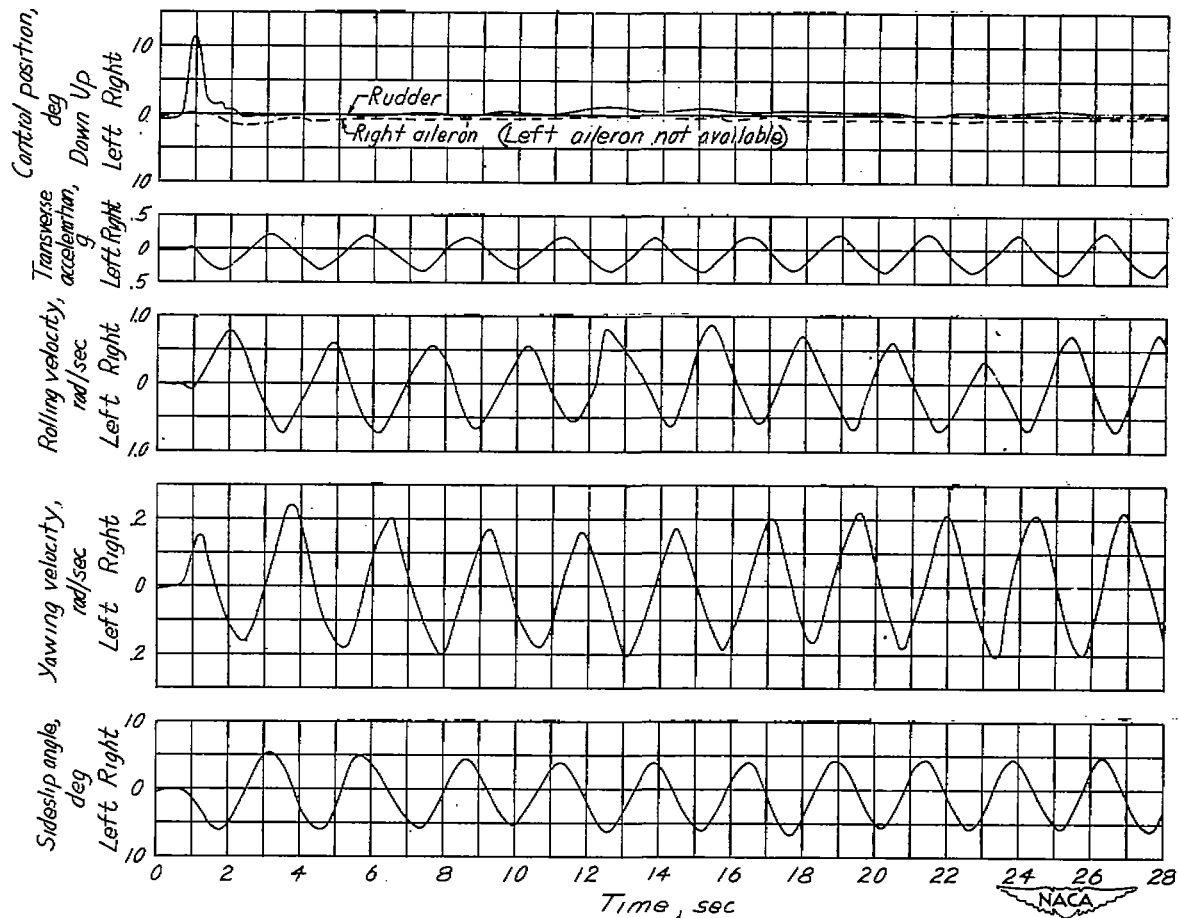


Figure 14.- Time history of a control-fixed lateral oscillation of the D-558-II (BuAero No. 37974) research airplane. Flaps down; landing gear down; slats unlocked; $V_c = 229$ miles per hour; $H = 16,400$ feet; $C_{N_A} = 0.40$.

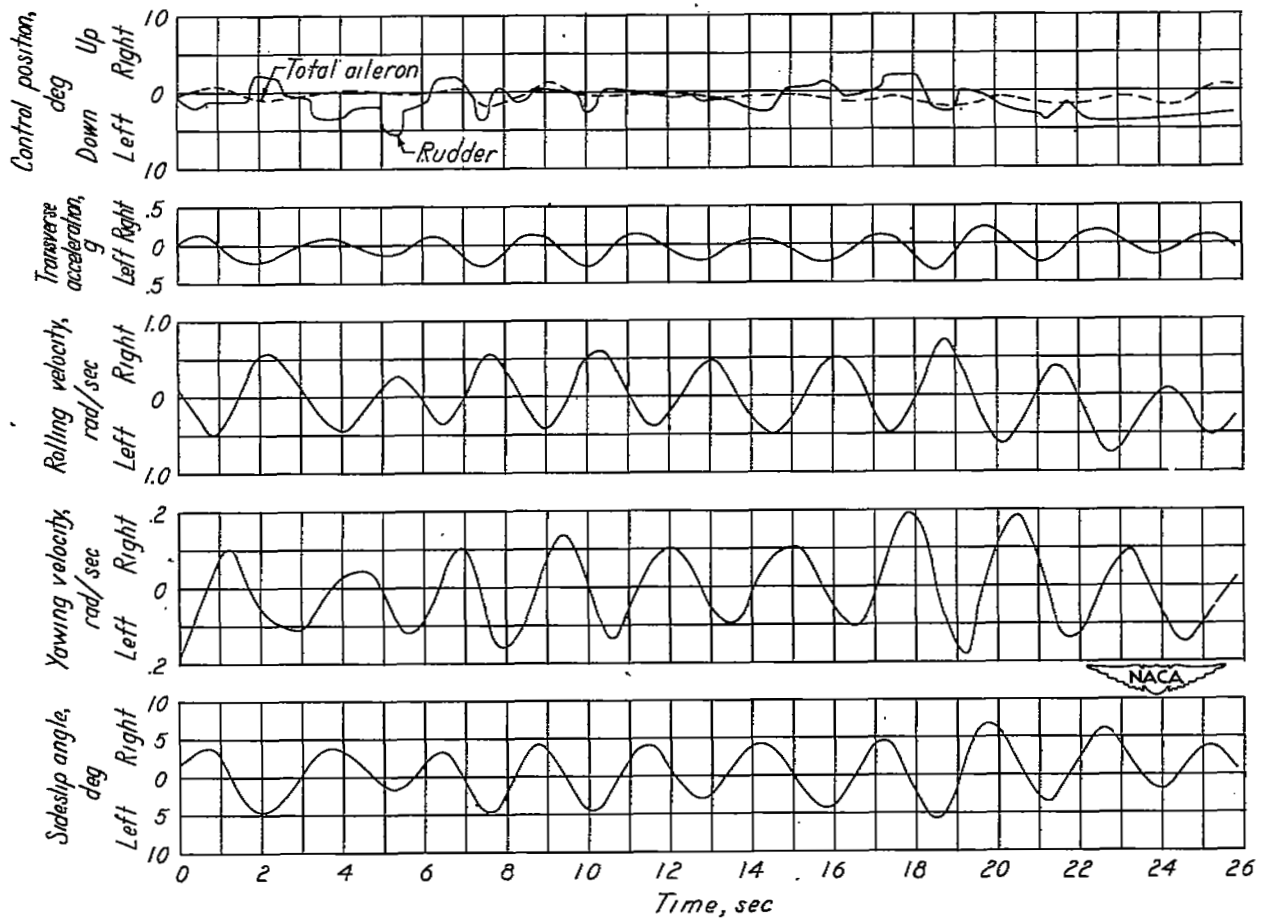


Figure 15.- Time history of a lateral oscillation of the D-558-II (BuAero No. 37974) research airplane, with the pilot using control to attempt to stop the oscillation. Flaps down; landing gear down; slats unlocked; $V_c = 237$ miles per hour; $H = 7,200$ feet; $C_{N_A} = 0.37$.

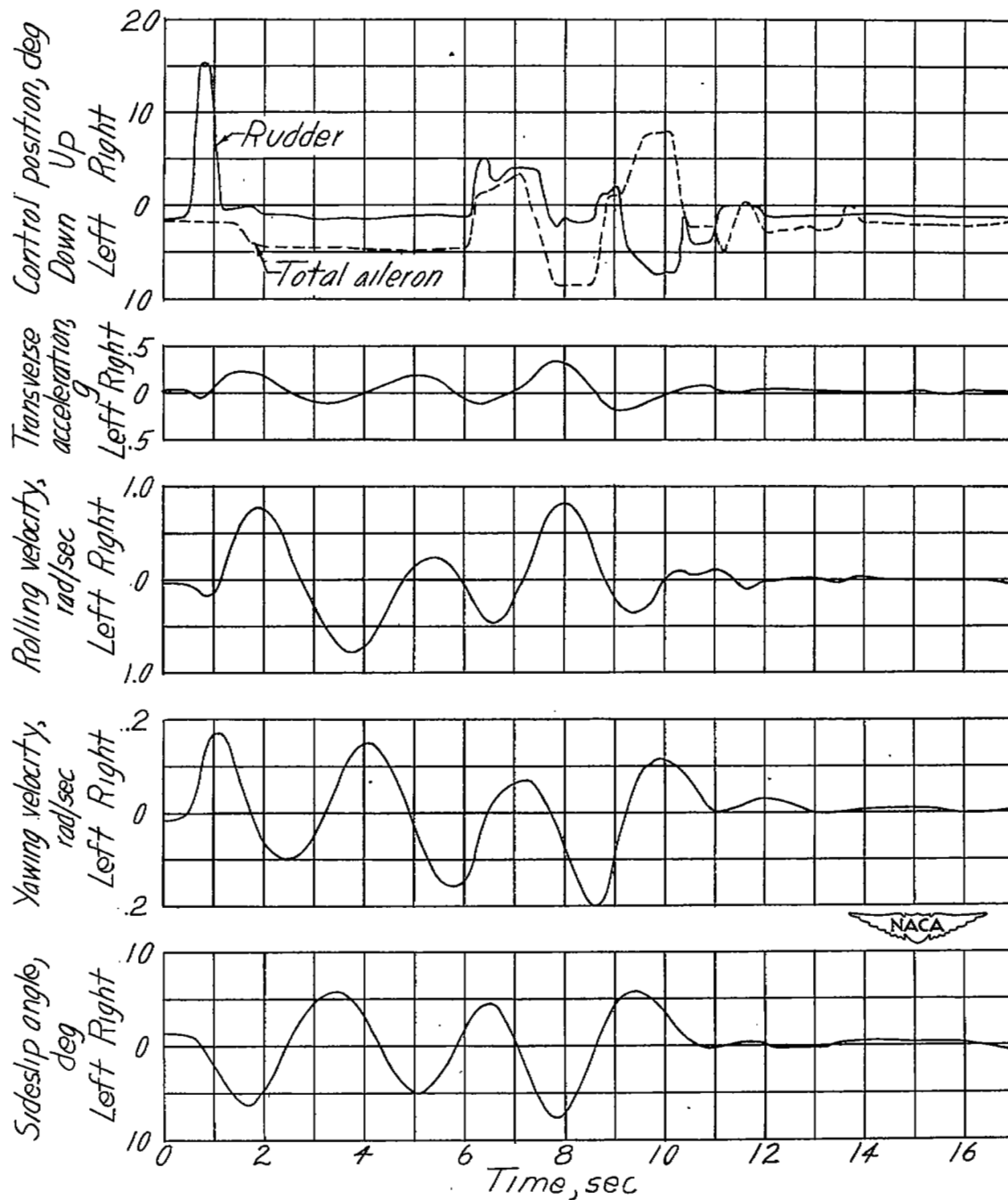


Figure 16.- Time history of a lateral oscillation of the D-558-II (BuAero No. 37974) research airplane, with the pilot using control to stop the oscillation. Flaps down; landing gear down; slats unlocked; $V_C = 205$ miles per hour; $H = 8,600$ feet; $C_{N_A} = 0.50$.

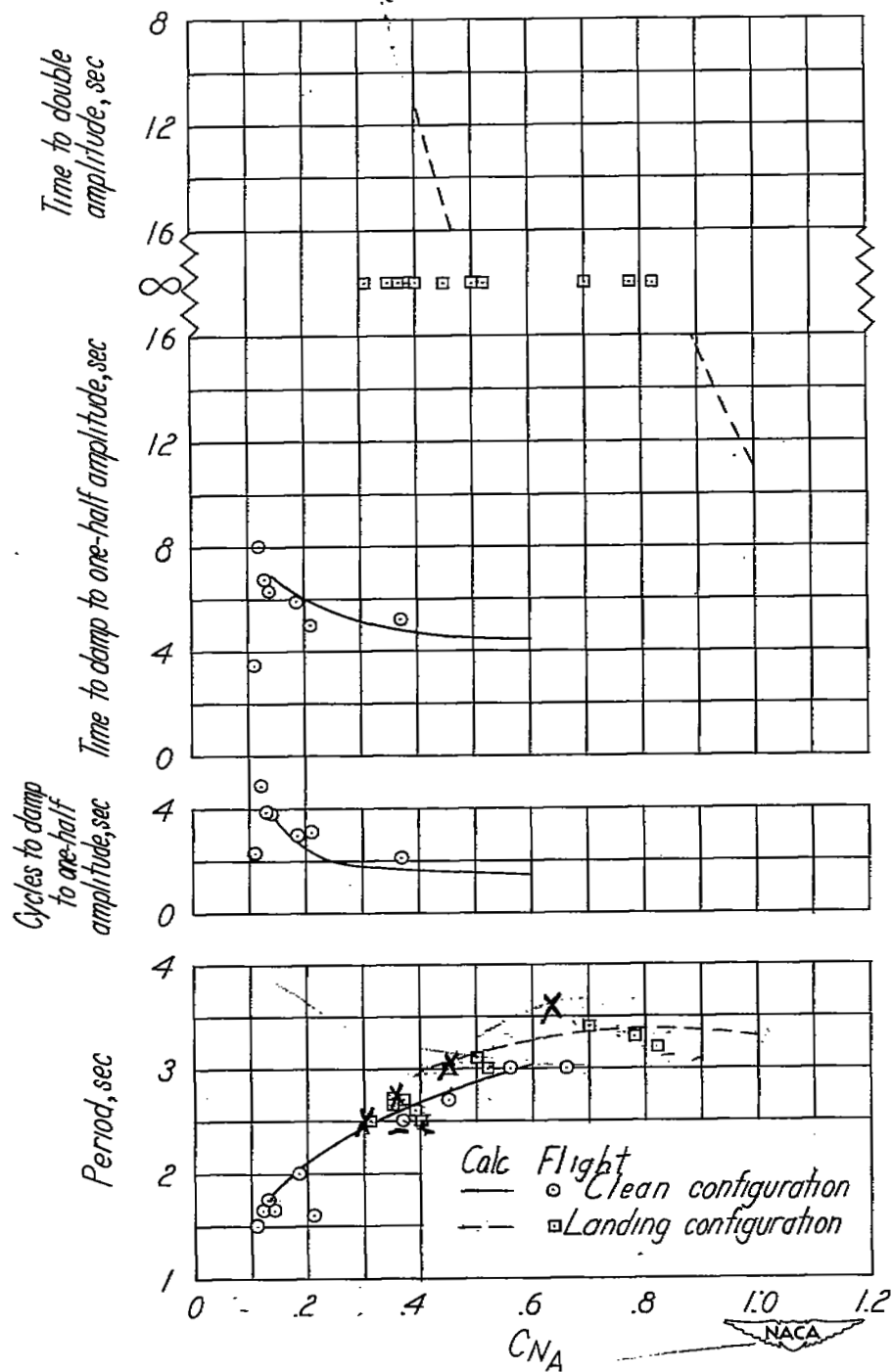


Figure 17.- Variation of period and damping characteristics with normal-force coefficient of the lateral oscillation of the D-558-II (BuAero No. 37974) research airplane.

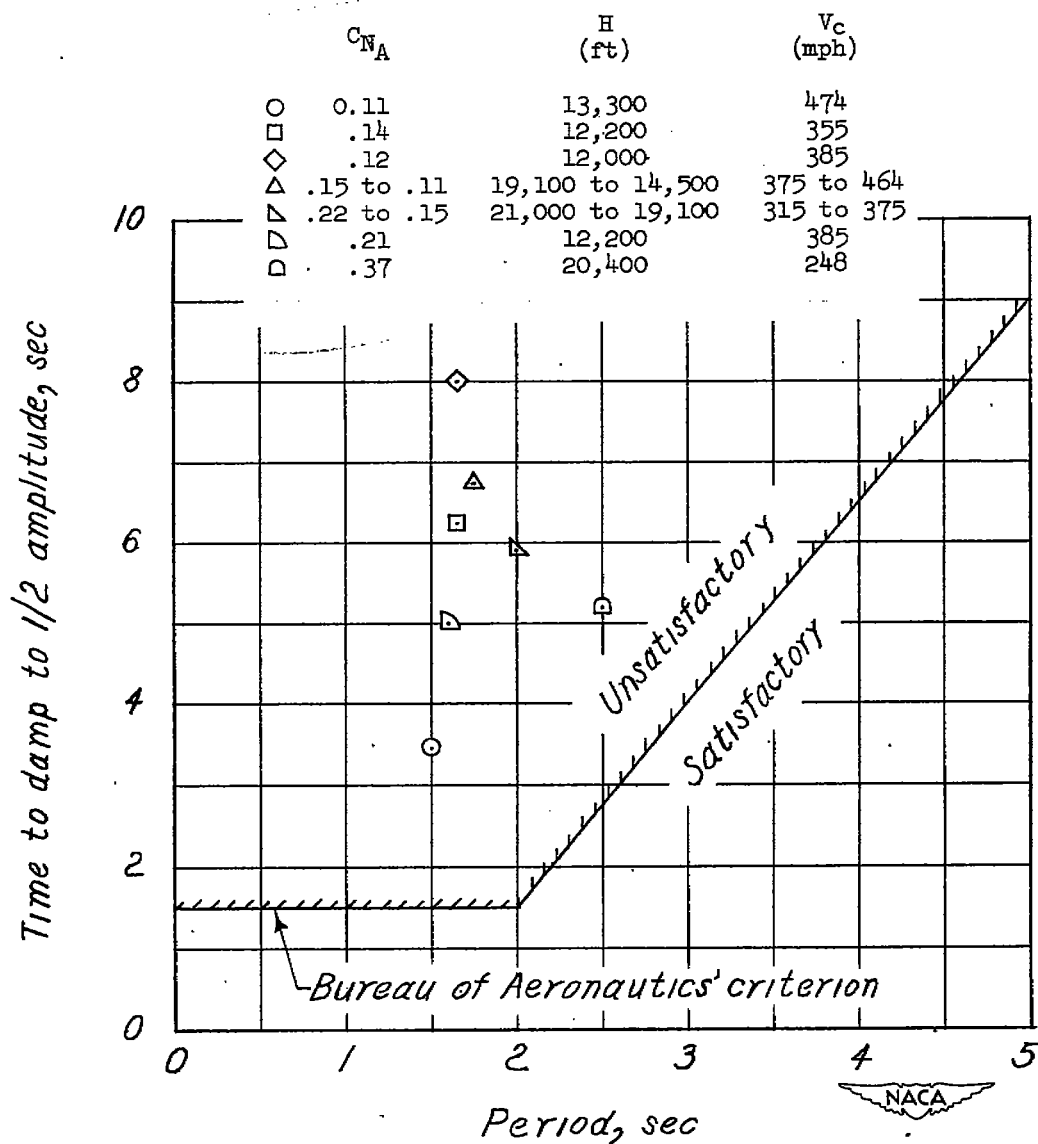


Figure 18.- Period damping characteristics of the lateral oscillation of the D-558-II (BuAero No. 37974) research airplane in the clean condition.

NASA Technical Library



3 1176 01436 8543

